Journal of Alloys and Compounds 500 (2010) 149–152

Contents lists available at ScienceDirect

Journal of Alloys and Compounds

journal homepage: www.elsevier.com/locate/jallcom

Preparation and size-modulation of silica-coated maghemite nanoparticles

M.P.S. de Almeida[a], K.L. Caiado[a], P.P.C. Sartoratto[a,*], D.O. Cintra e Silva[b], A.R. Pereira[c], P.C. Morais[d]

[a] Universidade Federal de Goiás, Instituto de Química, Goiânia, GO 74001-970, Brazil
[b] Universidade de Brasília, Instituto de Ciências Biológicas, Brasília, DF 70910-900, Brazil
[c] Universidade Federal de Goiás, Unidade Catalão, GO 75704-020, Brazil
[d] Universidade de Brasília, Instituto de Física, Brasília, DF 70910-900, Brazil

ARTICLE INFO

Article history:
Received 10 July 2008
Received in revised form 20 October 2009
Accepted 28 October 2009
Available online 5 November 2009

Keywords:
Nanostructured materials
Surfaces and interfaces
Chemical synthesis

ABSTRACT

In this study we report on the synthesis and characterization of both silica-coated and aminopropyl-silica-coated maghemite nanoparticles of different particle sizes by one-step reaction of an alkaline aqueous-based dispersion of maghemite nanoparticles (7–10 nm). The nanoparticle surface coating was performed using tetraethoxysilane. The influence of reaction time, amount of maghemite nanoparticles and tetraethoxysilane employed in the synthesis upon the composition and morphology of the as-prepared samples and on the colloidal dispersion properties produced from them was investigated. The weight percentage of silica in the composite samples varied from 5.4 to 94% depending on reaction conditions. When very low amount of maghemite nanoparticles is present in the reaction mixture, large and nearly spherical-shaped multicore maghemite–silica particles (60–80 nm) are predominantly formed. On the other hand, when high amounts of maghemite nanoparticles are employed, smaller core–shell particles and non-spherical aggregates of them were observed. The silica-coated maghemite particles showed negative zeta potential values for their neutral aqueous dispersions while improved colloidal stability (stable magnetic fluid samples) was observed for small-sized suspended particles. In turn, the aminopropyl-silica-coated maghemite particles showed positive zeta potential values greater than +30 mV only for acidic aqueous dispersions and the colloidal stability also varied according to the particle size.

1. Introduction

A wide variety of applications involving superparamagnetic iron oxide (SPIO) particles are related to stable colloidal dispersions of nanosized particles in a continuous liquid phase named magnetic fluid (MF). Each particular application demands nanoparticle's production with specific characteristics, taking into account the chemical and structural stabilities of the core as well as the physico-chemical properties of the shell. The nanoparticle shell plays multiple functions, such as protecting the magnetic core against phase changes, improving colloidal stability, and incorporating surface functionality. Furthermore, the presence of reactive chemical groups on the nanoparticle surface allows for instance conjugation of biomolecules, fluorescent probes, and drugs. Silica and organo-functionalized silica have been pointed out as a convenient surface coating for SPIO particles [1,2]. Typically, there are two methods to prepare silica-coated magnetite or maghemite particles. One of them is based on a microemulsion approach using tetraethoxysilane [3–5] and the other is based on the Stöber process in which silica is formed by the hydrolysis and condensation of tetraethoxysilane in an aqueous solution containing ethanol and ammonia [6]. The method based on the Stöber process was described by Philipse [7] who found to be necessary to firstly deposit a thin silica layer onto the nanoparticle surface using a water glass solution before reacting them with the tetraethoxysilane precursor mixture. Variations of this method continue to be explored and studied recently by other authors [8–12].

In this study we report on the successful synthesis of silica-coated maghemite (SM) nanoparticles of different particle sizes by a one-step reaction of alkaline aqueous dispersion of maghemite nanoparticles with a solution of tetraethoxysilane in ethanol. Aminopropyl-silica-coated maghemite (ASM) nanoparticles were obtained from the reaction of the previously prepared SM samples with 3-aminopropytrimethoxysilane. The influence of the synthesis parameters on the characteristics of the as-prepared samples and on the colloidal dispersions properties produced from them was also investigated.

2. Experimental procedures

Silica-coated maghemite (SM) and aminopropyl-silica-coated maghemite (ASM) nanoparticles were prepared employing a modification of the Stöber method

* Corresponding author. Tel.: +55 62 35211016; fax: +55 62 35211167.
E-mail addresses: patricia@quimica.ufg.br, patconf@gmail.com (P.P.C. Sartoratto).

0925-8388/$ – see front matter © 2009 Elsevier B.V. All rights reserved.
doi:10.1016/j.jallcom.2009.10.245

using tetraethoxysilane (TEOS) and 3-aminopropyltrimethoxysilane (APTMS), water, ethanol, and ammonium hydroxide. The maghemite nanoparticles were introduced into the reaction mixture as aqueous MF samples which were previously prepared. The influence of the reaction time, amount of nanoparticles and TEOS employed in the synthesis upon the characteristics of the SM and ASM samples was investigated.

Maghemite nanoparticle samples were obtained by bubbling oxygen in an acid (pH = 3.5) aqueous suspension containing magnetite nanoparticles, at 90 °C for 6 h. Magnetite was synthesized by chemical co-precipitation of Fe(II) and Fe(III) ions in alkaline medium, following a procedure described in the literature [13]. In each case, the solids were isolated by centrifugation and washed several times with acetone/water. Aqueous-based maghemite MF samples (pH = 5) were prepared by peptizing maghemite nanoparticles in water followed by dialysis in deionized water. The total concentration of iron in the maghemite-based MF samples varied in the range of 1.0–1.5 mol L^{-1}, as determined from atomic absorption analysis. The amount of residual Fe(II) within the samples was determined by the orthophenantroline spectrophotometric method. Powder X-ray diffraction of maghemite samples was recorded in a Schimadzu XRD 6000 equipment, using the Cu-Kα radiation. The X-ray line broadening of the most intense diffraction peak (3 1 1) of the cubic spinel diffraction pattern provided the average diameter (7–10 nm) of the nanocrystalline domain for the maghemite prepared samples. The average nanoparticle size was estimated using the Scherrer's equation [14,15].

The synthesis apparatus used to prepare the SM samples consisted on a two-necked round-bottom flask coupled with a condenser and an addition funnel. A typical procedure consisted on adding a solution containing ethanol and TEOS to the aqueous-based maghemite MF sample containing ammonium hydroxide (pH 8.5–9.0). The suspension was stirred at room temperature for periods of time that varied from 4 to 24 h. The preparation of ASM samples consisted on adding an aqueous solution of APTMS to the previously prepared suspension of maghemite/silica particles. The solids were isolated by centrifugation, washed several times with ethanol and water and finally suspended in water. Table 1 shows the details regarding the reaction conditions and sample identification.

The diffuse reflectance infrared spectra (DRIFTS) of composite samples were obtained in a FTIR Bomem, MB 100 equipment, with samples dispersed in KBr (1%). Taking into account the iron content obtained from atomic absorption analysis and considering that all silicon were present as SiO_2 the silica content (weight%) within the composite samples (heated at 120 °C until weight was constant) was estimated after digestion of solid samples in hot hydrochloric acid. Hydrodynamic radius and zeta potential of diluted aqueous dispersions of MF (pH = 5), SM (pH = 7) and ASM (pH = 3) samples were determined by dynamic light scattering measurements using a Malvern Instrument Zeta Sizer Nano Series ZS90. Samples were also analyzed by transmission electron microscopy (TEM) in a Jeol JEM 1011 instrument. All measurements were done at room temperature.

3. Results and discussion

The powder X-ray diffraction patterns of maghemite and maghemite–silica composite samples show the typical X-ray peaks of the maghemite spinel structure (JCPDF 25-1402), with lattice parameter values between those for bulk maghemite (0.839 nm) and bulk magnetite (0.834 nm). All iron oxide samples prepared in this study contained around 5% Fe (II).

Fig. 1 shows the FTIR spectra of the SM and ASM samples in the 1300–500 cm^{-1} region. All spectra show the γ-Fe_2O_3 bands at 636 and 582 cm^{-1} [16], the superimposed asymmetric Si–O–Si stretching bands at around 1080 and 1180 cm^{-1}, plus the symmetric Si–O–Si stretching band around 800 cm^{-1}. The asymmetric Si–O stretching band of Si–OH groups peaks around 960 cm^{-1} [17]. The intensities of the Si–O–Si and Si–OH bands compared to those of the γ-Fe_2O_3 bands varied significantly, indicating samples containing different amounts of silica [18]. Furthermore, the shape of the asymmetric Si–O–Si stretching bands changes according to the sample's preparation condition. The lower frequency band around 1100 cm^{-1} is usually attributed to the vibration mode of perfect SiO_4 tetrahedra whereas the higher frequency band around 1200 cm^{-1} is due to distorted SiO_4 [19]. The asymmetric Si–O–Si absorptions for the SM/TS1 sample that contains lower silica content seems to be enlarged and shifted to lower frequencies, suggesting a less interconnected silica network that still contains some amount of non-hydrolyzed –$SiOCH_2CH_3$ groups. The ASM/1 sample shows other bands in the 1300–1600 cm^{-1} region (not shown) associated to aminopropyl groups [20]. Table 1 shows the results of the light scattering measurements together with the estimative of the silica content. The weight percentage of silica varied from 5.4 to 80% for the SM samples depending on reaction conditions. Considering samples of the series SM/T which were obtained from a fixed H_2O:NH_3:CH_3CH_2OH:TEOS molar proportion, it can be noted that the reaction time had a significant effect on the sample composition. The silica amount for sample SM/T2 (reaction time of 8 h) was about twice that for sample SM/T1 (reaction time of

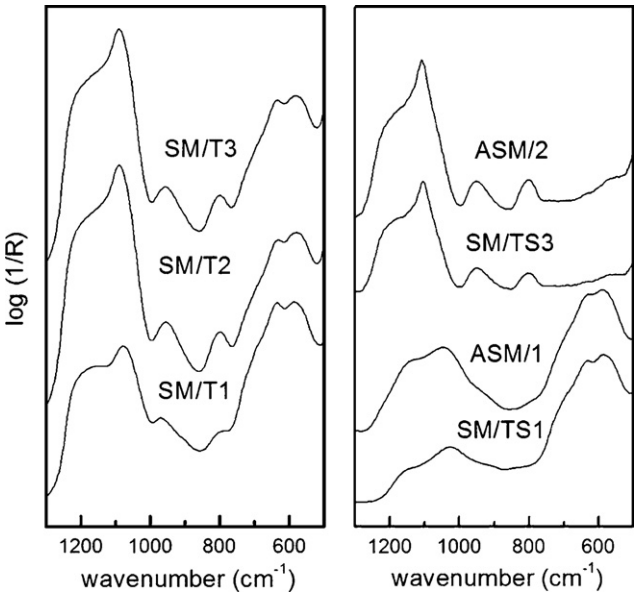

Fig. 1. DRIFTS spectra of the silica-coated maghemite and aminopropyl-silica-coated maghemite samples.

Table 1
Maghemite nanocrystallite average diameter (D_{XRD}), reaction conditions, silica content of the composite particles, average hydrodynamic radius (Rh), polydispersion index (PDI) and zeta potential (ζ) for the aqueous dispersions of silica-coated maghemite (SM) and aminopropyl-silica-coated nanoparticles (ASM).

Sample	D_{XRD} (nm)	NP/TEOS[a] (10^{16} mL^{-1})	H_2O:NH_3:CH_3CH_2OH:TEOS (mol)	Reaction time (h)	SiO_2 (wt%)	Rh (PDI) (nm)	ζ (mV)
SM/P1	7	3	54:0.1:41:1.0	24	39	79 (0.23)	−35.8
SM/P2	7	10	54:0.1:41:1.0	24	20	74 (0.19)	−43.3
SM/T1	8	8	54:0.1:41:1.0	4	22	98 (0.19)	−40.1
SM/T2	8	8	54:0.1:41:1.0	8	46	172 (0.36)	−37.4
SM/T3	8	8	54:0.1:41:1.0	12	51	170 (0.32)	−37.1
SM/TS1	10	110	54:0.1:41:0.062	4	5.4	90 (0.17)	−44.1
SM/TS2	10	11	54:0.1:41:0.620	4	10	170 (0.40)	−38.6
SM/TS3[b]	9	0.1	59:1.9:153:1.0	24	80	–	–
ASM/1	SM/TS1	8.6[c]	–	4	15	76 (0.19)	+37.8
ASM/2	SM/TS3	1.2[c]	–	24	94	82 (0.07)	+65.9

[a] The average number of maghemite nanoparticles (NP) in MF samples was estimated from the iron content, average nanoparticle size (XRD), and bulk maghemite density.
[b] Colloidal stability of SM/TS3 aqueous dispersion was very poor and light scattering measurements could not be done.
[c] Weight (g) of SM sample to the volume (mL) of APTMS.

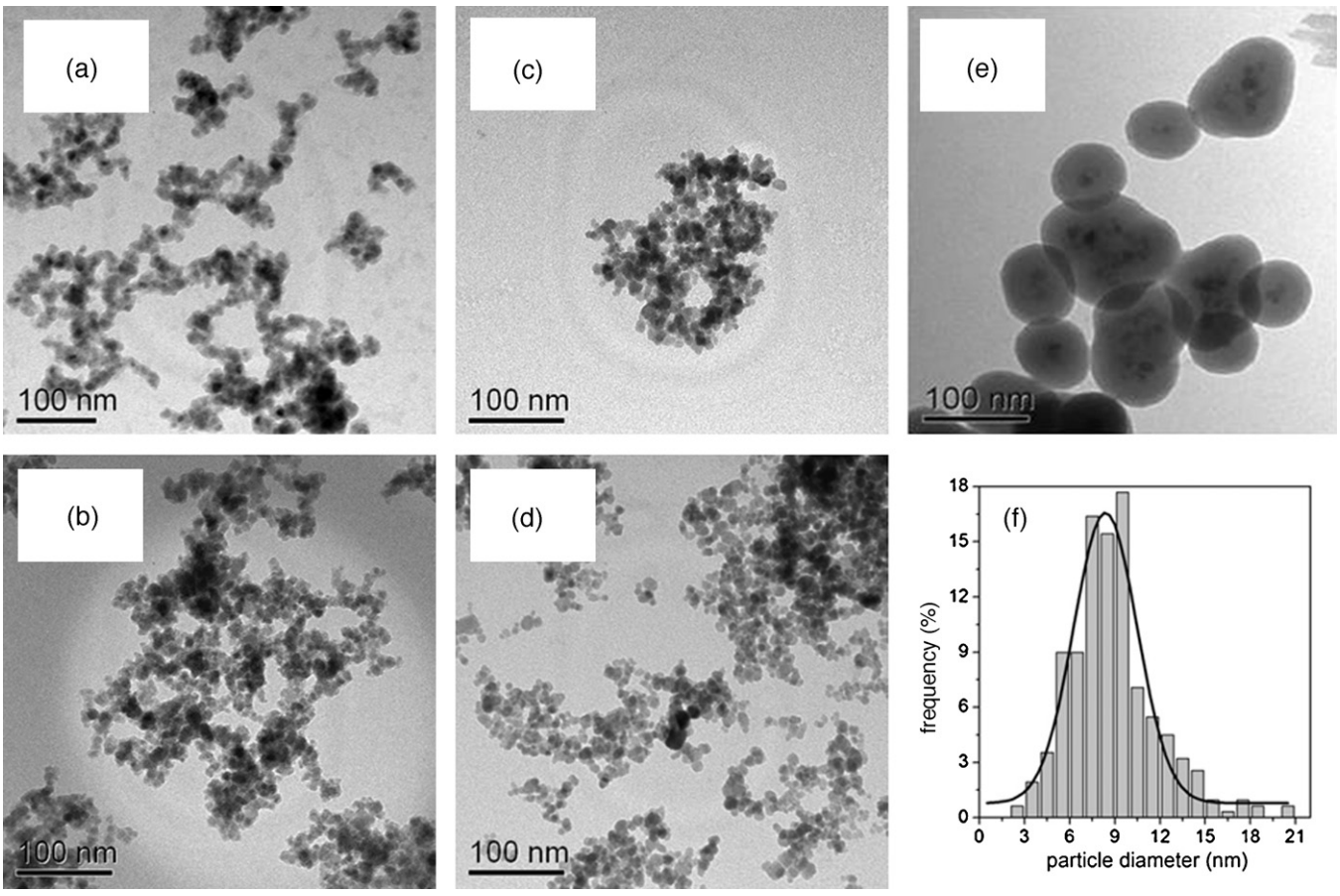

Fig. 2. TEM images of samples SM/P1 (a), SM/P2 (b), SM/TS1 (c), ASM/1 (d), ASM/2 (e), and particle size histogram of sample ASM/1 (f).

4 h). However, the silica percentage showed just a small increment when the reaction time was increased to 12 h (sample SM/T3). Considering samples of the series SM/P which were also obtained from the same reagent proportions but with different NP/TEOS ratios, it can be noted that as the ratio of amount of nanoparticles to the volume of TEOS increases the silica content decreases. The same tendency regarding the relation between silica content and NP/TEOS ratio employed in the synthesis was observed for SM/TS samples despite the fact they were prepared from very different H_2O:NH_3:CH_3CH_2OH:TEOS molar proportions and reaction times. Sample SM/TS1 contains only 5.4% of silica whereas sample SM/TS3 showed 80% of silica. As expected, samples ASM/1 and ASM/2 presented higher silica contents than their precursor samples SM/TS1 and SM/TS3, respectively.

Except for sample SM/TS3, all the aqueous dispersions of SM samples (pH = 7) presented higher colloidal stability, as can be verified by the zeta potentials in the range of −35.8 to −43.3 mV (see Table 1). Sample SM/TS3 showed reduced stability; the particles suspended in water (pH = 7) being decanted very rapidly, suggesting the presence of bigger particles with high weight and low surface charge density. MF samples (pH = 5) used to prepare these SM particles showed positive zeta potentials around +40 mV due to Fe–OH_2^+ species at the maghemite nanoparticle surface [21]. Thus the negative potential observed for the SM samples evidences the presence of Si–O^- species on the surface of the SM particles. The average hydrodynamic radius (Rh) of SM particles varied from 74 to 172 nm, the size distribution being monomodal and broad with polydispersion index (PDI) between 0.17 and 0.40. For samples SM/T1 and SM/T2 the Rh increases with the increasing of the silica content. However, samples SM/P1 and SM/P2 showed similar Rh values despite their different silica contents. Zeta potentials for the aqueous dispersions of ASM samples (pH = 3) were positive suggesting the presence of protonated amine groups on the particle's surface. Sample ASM/2 showed the highest potential value of +65.9 mV, average Rh value of 82 nm, and a narrower distribution of hydrodynamic radius as indicated by the low PDI value of 0.065. Above pH = 3 the colloidal stability of the ASM samples was very poor due to the low surface charge density.

Fig. 2 shows the TEM images of SM and ASM samples. The morphology of samples SM/P1 and SM/P2 is very similar, presenting some individual maghemite nanoparticles (around 5–10 nm) covered by a very thin silica layer (around 2–3 nm). In addition to individual nanoparticles bigger structures with non-spherical morphology were also observed, more likely coming from aggregation/coalescence of individual nanoparticles. Although sample SM/P2 also contains the above-mentioned non-spherical structures it seems that they are smaller than the ones observed in sample SM/P1. The TEM average diameters of composite particles were respectively 11 ± 2 and 9 ± 2 nm for samples SM/P1 and SM/P2 whereas the XRD average diameter of the precursor maghemite nanoparticle was 7 nm. Although the particle sizes obtained from the XRD measurements are usually bigger than those determined via TEM the small increase in the average diameter of the composite particles as obtained by TEM strongly indicates that the maghemite nanoparticles are covered by a thin layer of silica. Thus, the formation of aggregates in the aqueous dispersion of these particles may explain the high Rh values determined by the dynamic light scattering measurements.

It may be argued that for a NP/TEOS ratio below 3, as employed in the synthesis of sample SM/P1, the formation of aggregates of primary maghemite–silica particles is favored. It is worth to

note that sample SM/TS1, which was prepared using a very high NP/TEOS ratio of 110 from a more dilute reaction medium and a short reaction time, did not shows large aggregates (Fig. 2(c)). The aqueous dispersion of this sample also shows a high Rh value (90 nm) despite the value of TEM diameter (D_{TEM}) being only 8 ± 1 nm. Again, this finding suggests that aggregation is important in aqueous medium. On the other hand sample SM/TS3, which was prepared using a very low NP/TEOS ratio of 0.1 from a reaction mixture that contained higher amount of ethanol and ammonia, mainly presents large multicore maghemite–silica particles (60–80 nm), with nearly spherical shape and showing a thicker silica layer (Fig. 2(e)). However, this sample also contains larger particles of up to 200 nm in size, which seems to have been formed from the coalescence of smaller ones. The morphologies of the ASM/1 and ASM/2 samples are very similar to the ones observed for SM/TS1 and SM/TS3, respectively. The D_{TEM} value for the ASM/1 (9 ± 1 nm) sample was slightly higher than the value for the SM/TS1 (8 ± 1 nm) sample, as expected. However, an opposite trend occurred with the Rh values, probably due to the presence of different functionalities on the particles' surface. Thus, the reaction of APTMS onto the previously prepared SM particles does not promote any further aggregation.

These findings can be understood in terms of a model described in the literature for the method described by Philipse [7] regarding the preparation of micrometer magnetite–silica particles. Following this route maghemite nanoparticles are firstly coated with a very thin layer of silica using a silicate solution. These primary particles aggregate in aqueous solution containing ethanol and ammonia and then TEOS is added into the reaction mixture, resulting in the formation of spherical multicore maghemite–silica particles with sizes that vary in the range of 0.5–10 μm. In the method used in the present study TEOS was directly poured into an alkaline aqueous dispersion of maghemite nanoparticles, with no previous particle coating. It is important to emphasize that maghemite nanoparticles remained dispersed during the entire synthesis; no flocculation being noted by visual inspection. This is interesting because other authors observed flocculation for similar reaction conditions [8]. The difference observed here may be associated with the fact that the MF samples employed in our synthesis were dialyzed for many days to reduce excess ions and charges and the pH was carefully raised to 8.5–9.0 by adding ammonium hydroxide. When the amount of TEOS used in the synthesis is low (NP/TEOS = 3–10) the hydrolyzed and partially condensed TEOS formed at the early stages of reaction deposit on the maghemite nanoparticles and onto the small aggregates of them, resulting in primary maghemite–silica particles of small sizes. These small primary particles may aggregate and coalesce randomly in a low TEOS concentration medium so that the further growth of the silica layer is not favored. On the other hand, when the amount of TEOS is high (NP/TEOS = 0.1) the primary maghemite–silica particles may also form and aggregate, but the growth of the silica layer on the surface of these aggregates is enhanced due to the high concentration of TEOS, resulting in multicore maghemite–silica particles with a silica layer of large thickness. Furthermore, when the amount of TEOS used in the synthesis is very low (NP/TEOS = 110) most of the partially hydrolyzed TEOS that is present in the early stages of the reaction is incorporated onto the surface of the maghemite nanoparticles, so that a very thin and less interconnected silica network layer is formed around maghemite nanoparticles. In this case, the density of negative charges on the maghemite–silica particles may be large enough to inhibit extensive aggregation.

4. Conclusion

The one-step reaction of alkaline aqueous dispersion of maghemite nanoparticles with tetraethoxysilane resulted in silica-coated maghemite nanoparticles, which were successfully used to further prepare aminopropyl-silica-coated maghemite nanoparticles. The weight percentage of silica within the samples could be tuned by varying the synthesis parameters such as the reaction time and the amount of maghemite nanoparticles and tetraethoxysilane, which also determined whether large multicore silica–maghemite composite particles, small core–shell particles or aggregates of them predominate in the as-prepared samples. The colloidal stability of the aqueous dispersions of the prepared samples varied according to the pH of the medium, nature of chemical groups at the particle's surface, and size of the composite particles. The small core–shell composite nanoparticles that contain a very thin layer of silica or aminopropyl-silica is useful to obtain stable magnetic fluids, whereas the large multicore composite particles can be employed as magnetic beads. Further improvements in synthetic strategies are in progress in order to prepare maghemite–silica and maghemite–aminopropyl-silica core–shell particles of variable sizes with avoidable aggregation.

Acknowledgments

This work was partially supported by the Brazilian agencies FUNAPE, FINATEC, and MCT/CNPq.

References

[1] T.J. Yoon, J.S. Kim, B.G. Kim, K.N. Yu, M.H. Cho, J.K. Lee, Angew. Chem. Int. Ed. 44 (2005) 1068–1071.
[2] Q.A. Pankhurst, J. Connolly, S.K. Jones, J. Dobson, J. Phys. D: Appl. Phys. 36 (2003) 167–181.
[3] K. Landfester, L.P. Ramírez, J. Phys.: Condens. Matter 15 (2003) 1345–1361.
[4] C.R. Vestal, Z.J. Zhang, Nano Lett. 3 (2003) 1739–1743.
[5] S. Santra, R. Tapec, N. Theodoropoulou, J. Dobson, A. Hebard, W. Tan, Langmuir 17 (2001) 2900–2906.
[6] W. Stöber, A. Fink, J. Colloid Interface Sci. 26 (1968) 62–69.
[7] A.P. Philipse, M.P.B. van Bruggen, C. Pathmamanoharan, Langmuir 10 (1994) 92–99.
[8] Z. Lu, J. Dai, X. Song, G. Wang, W. Yang, Colloid Surf. A: Physicochem. Eng. Aspects 317 (2008) 450–456.
[9] I.J. Bruce, T. Sen, Langmuir 21 (2005) 7029–7035.
[10] I.J. Bruce, J. Taylor, M. Todd, M.J. Davies, E. Borioni, C. Sangregorio, T. Sen, J. Magn. Magn. Mater. 284 (2004) 145–160.
[11] P. Tartaj, M.D. Morales, S.V. Verdaguer, T.G. Carrenõ, C.J. Serna, J. Phys. D: Appl. Phys. 36 (2003) R182–R197.
[12] Z. Lu, G. Wang, J. Zhuang, W. Yang, Colloid Surf. A: Physicochem. Eng. Aspects 278 (2006) 140–143.
[13] Y.S. Kang, S. Risbud, J.F. Rabolt, P. Stroeve, Chem. Mater. 8 (1996) 2209–2211.
[14] B.D. Cullity, Elements of X-ray Diffraction, Addison-Wesley, Canada, 1978.
[15] P.C. Morais, E.C.D. Lima, D. Rabelo, A.C. Reis, F. Pelegrini, IEEE Trans. Magn. 36 (2000) 3038–3040.
[16] S.L. Tie, H.C. Lee, Y.S. Bae, M.B. Kim, K. Lee, C.H. Lee, Colloid Surf. A: Physicochem. Eng. Aspects 293 (2007) 278–285.
[17] S. Bruni, F. Cariati, M. Casu, A. Lai, A. Musinu, G. Piccaluga, S. Solinas, Nanostruct. Mater. 11 (1999) 573–586.
[18] P.P.C. Sartoratto, K.L. Caiado, R.C. Pedroza, S.W. da Silva, P.C. Morais, J. Alloys Compd. 434–435 (2007) 650–654.
[19] F. Balas, M. Rodrígues-Delgado, C. Otero-Arean, F. Conde, E. Matesanz, L. Esquivias, J. Ramírez-Castellanos, J. Gonzalez-Calbet, M. Vallet-Regí, Solid State Sci. 9 (2007) 351–356.
[20] S. Mohapatra, N. Pramanik, S. Mukherjee, S.K. Ghosh, P. Pramanik, J. Mater. Sci. 42 (2007) 7566–7574.
[21] P.C. Morais, S.W. da Silva, M.A.G. Soler, N. Buske, Biomol. Eng. 17 (2001) 41–49.